
A Phase 1, Open-Label Study of the Biodistribution, Pharmacokinetics, and Dosimetry of ^{223}Ra -Dichloride in Patients with Hormone-Refractory Prostate Cancer and Skeletal Metastases

Sarah J. Chittenden¹, Cecilia Hindorf², Christopher C. Parker³, Valerie J. Lewington⁴, Brenda E. Pratt¹, Bernadette Johnson³, and Glenn D. Flux¹

¹Joint Department of Physics, Royal Marsden Hospital and Institute of Cancer Research, Sutton, Surrey, United Kingdom; ²Department of Radiation Physics, Radionuklidcentralen, Skåne University Hospital Lund, Lund, Sweden; ³Department of Urology, Royal Marsden Hospital, Sutton, Surrey, United Kingdom; and ⁴Department of Nuclear Medicine, Guy's Hospital, London, United Kingdom

The aim of this single-site, open-label clinical trial was to determine the biodistribution, pharmacokinetics, absorbed doses, and safety from 2 sequential weight-based administrations of ^{223}Ra -dichloride in patients with bone metastases due to castration-refractory prostate cancer.

Methods: Six patients received 2 intravenous injections of ^{223}Ra -dichloride, 6 wk apart, at 100 kBq/kg of whole-body weight. The pharmacokinetics and biodistribution as a function of time were determined, and dosimetry was performed for a range of organs including bone surfaces, red marrow, kidneys, gut, and whole body using scintigraphic imaging; external counting; and blood, fecal, and urine collection. Safety was assessed from adverse events. **Results:** The injected activity cleared rapidly from blood, with 1.1% remaining at 24 h. The main route of excretion was via the gut, although no significant toxicity was reported. Most of the administered activity was taken up rapidly into bone (61% at 4 h). The range of absorbed doses delivered to the bone surfaces from α emissions was 2,331–13,118 mGy/MBq. The ranges of absorbed doses delivered to the red marrow were 177–994 and 1–5 mGy/MBq from activity on the bone surfaces and from activity in the blood, respectively. No activity-limiting toxicity was observed at these levels of administration. The absorbed doses from the second treatment were correlated significantly with the first for a combination of the whole body, bone surfaces, kidneys, and liver. **Conclusion:** A wide range of interpatient absorbed doses was delivered to normal organs. Inpatient absorbed doses were significantly correlated between the 2 administrations for any given patient. The lack of gastrointestinal toxicity is likely due to the low absorbed doses delivered to the gut wall from the gut contents. The lack of adverse myelotoxicity implies that the absorbed dose delivered from the circulating activity may be a more relevant guide to the potential for marrow toxicity than that due to activity on the bone surfaces.

Key Words: dosimetry; ^{223}Ra ; biodistribution; molecular radiotherapy; α -emitter

J Nucl Med 2015; 56:1304–1309

DOI: 10.2967/jnumed.115.157123

Prostate cancer is the most common male cancer worldwide and one of the leading causes of cancer-related morbidity and death. Castration-resistant prostate cancer has a poor prognosis, with a median survival of approximately 2 y. The limited treatment options available have done little to change the overall prognosis, and cytotoxic treatments are associated with substantial side effects. Approximately 90% of men with castration-resistant prostate cancer have radiologic evidence of bone metastases, which are the main cause of disability and death (1–4).

Several β -emitting radiopharmaceuticals, including ^{89}Sr -chloride, ^{186}Re -hydroxyethylidene disphosphonate, and ^{153}Sm -ethylene diamine tetramethylene phosphonate, have been developed for palliation of bone pain due to metastases (5). These radiopharmaceuticals target the increased metabolism in areas of bone tumor and have demonstrated preferential uptake in metastases relative to normal bone. α -emitting radiopharmaceuticals are increasingly under evaluation and offer highly localized cytotoxic effects due to their short range and high linear energy transfer (6,7). ^{223}Ra -dichloride is a novel, bone-seeking α emitter that has been administered to approximately 900 patients with bone metastases from castration-resistant prostate cancer in phase I–III clinical trials worldwide (8–14). It has demonstrated an antitumor effect on bone metastases in animal models (15). ^{223}Ra has a half-life of 11.4 d and decays via a chain of α and β emissions into stable lead. Although the proportion of γ emissions from each ^{223}Ra decay is only 1.1%, scanning and counting of patients and samples was shown to be feasible in a preliminary study to establish the basic parameters required for quantitative patient imaging of ^{223}Ra -dichloride (16).

To date, only 1 study has reported the radiopharmacokinetics of ^{223}Ra (12) based on clinical data, and 2 studies have calculated absorbed dose estimates based on the International Commission on Radiological Protection (ICRP) model for radium (17,18). However, to our knowledge, dosimetry results from a clinical study have not yet been published.

The primary aim of this phase 1 open-label clinical trial was to determine the biodistribution, pharmacokinetics, and dosimetry from 2 administrations of ^{223}Ra -dichloride (100 kBq/kg) administered 6 wk apart, based on the quantitative imaging methodology developed previously (16); external counting; and blood, urine, and fecal collection.

Received Mar. 5, 2015; revision accepted Jun. 23, 2015.
For correspondence or reprints contact: Sarah Chittenden, Physics Department, Royal Marsden NHS Hospital, Downs Rd., Sutton, Surrey, SM2 5PT, U.K.
E-mail: sarah.chittenden@icr.ac.uk
Published online Jul. 16, 2015.
COPYRIGHT © 2015 by the Society of Nuclear Medicine and Molecular Imaging, Inc.

TABLE 1
Patient Data

Characteristic	Patient no.					
	1	2	3	4	5	6
Age (y)	78	68	63	59	57	70
Weight (kg)						
Administration 1	72.5	64.8	74.5	97.6	110.0	78.9
Administration 2	72.7	65.2	77.6	97.4	110.6	79.5
Extent of disease (grade)*	1	2	4	2	3	4
Injected activity (kBq/kg)						
Administration 1	99	92	102	103	101	103
Administration 2	104	98	102	99	98	101

*Extent of disease grading system: 0, normal or abnormal because of benign bone disease; 1, fewer than 6 metastatic sites; 2, 6–20 metastatic sites; 3, more than 20 lesions but not a superscan; and 4, superscan.

MATERIALS AND METHODS

Patient Population

Six patients were enrolled into the study. Patients were assessed within 2 wk of ^{223}Ra administration and were included if all the following criteria were satisfied: confirmed adenocarcinoma of the prostate, hormone-refractory disease with evidence of rising prostate-specific antigen, serum testosterone level ≤ 50 ng/dL, skeletal metastases confirmed by bone scintigraphy, Eastern Cooperative Oncology Group performance status of 0–2, life expectancy ≥ 6 mo, neutrophils $\geq 1.5 \times 10^9/\text{L}$, platelets $\geq 100 \times 10^9/\text{L}$, hemoglobin ≥ 95 g/L, normal total bilirubin, aspartate aminotransferase and alanine aminotransferase ≤ 2.5 times the upper limit of the reference range

(ULN), and S-creatinine $\leq 1.5 \times \text{ULN}$, and the patient was able and willing to comply with the protocol and gave informed consent.

Patients were excluded for any of the following reasons: patient had received an investigational product in the 4 wk before ^{223}Ra administration or was scheduled to receive one during the study period; patient had received chemotherapy, immunotherapy, or external radiotherapy in the 4 wk before ^{223}Ra or was recovering from adverse events due to prior therapy; patient had previously received more than 1 regimen of cytotoxic chemotherapy; patient had prior hemibody radiotherapy; patient required immediate radiotherapy; patient had prior systemic radiotherapy with ^{223}Ra , ^{89}Sr , ^{153}Sm , ^{186}Re , or ^{188}Re ; bisphosphonates were started within 3 mo of ^{223}Ra (unless dosage stable for ≥ 12 wk before ^{223}Ra); patient had changes in systemic steroids within the week before ^{223}Ra or during study period; and patient had other active malignancies (except nonmelanoma skin cancer), visceral metastases from prostate cancer, lymph node metastases with short-axis diameter > 2 cm; bulky locoregional disease; and any other serious illness or medical condition.

This clinical trial (NCT00667537) was approved by the appropriate ethics committees and was conducted in accordance with the ethical standards laid down in the 1964 Declaration of Helsinki and its later amendments. All study subjects gave a signature of written informed consent.

Two intravenous injections of ^{223}Ra -dichloride were administered 6 wk apart at an activity of 100 kBq per kg of whole-body weight. Patients remained in the hospital for approximately 48 h after each administration, at which time they were discharged.

Data Acquisition

The biodistribution, pharmacokinetics, and absorbed doses were determined from activity retention measurements in the whole body, individual organs, blood, urine, and feces. Safety was assessed from adverse events, which were graded according to Common Terminology Criteria for Adverse Events (version 3.0) (19).

Blood Samples. Approximately 3 mL of blood were taken from a vein in the arm contralateral to the injection site. Samples were taken before injection; immediately after injection; then at 15, 30, and 45 min and 1, 2, 4, 24, 48, 96, and 144 h after injection. One milliliter of whole blood was taken from each blood sample. The sample was then centrifuged, and 1 mL of plasma removed. The 1 mL of blood and plasma samples was measured in an automatic γ counter. A 1-mL calibration standard containing a known activity of ^{223}Ra was counted with each set of samples.

Urine and Fecal Collection. A preinjection urine sample and first void after injection sample were collected separately. Thereafter, total urine output was collected separately for the time periods 0–4, 4–8, 8–24, and 24–48 h after injection. All feces excreted by each patient from injection to approximately 48 h were collected. Gamma spectroscopy of samples of urine and feces was performed using a whole-body counter, consisting of four 15-cm-diameter \times 10-cm-thick NaI(Tl) detectors in fixed geometry located in a shielded room. Corrections were made for dead-time and sample volume.

Whole-Body Measurements. Whole-body measurements of patients were performed on a low-sensitivity whole-body counter that consisted of a single NaI detector, photomultiplier tube, and preamplifier housed in a diverging lead collimator, suspended 2 m above a bed. The counting system had 1,024 channels over an energy range of 2,048 keV.

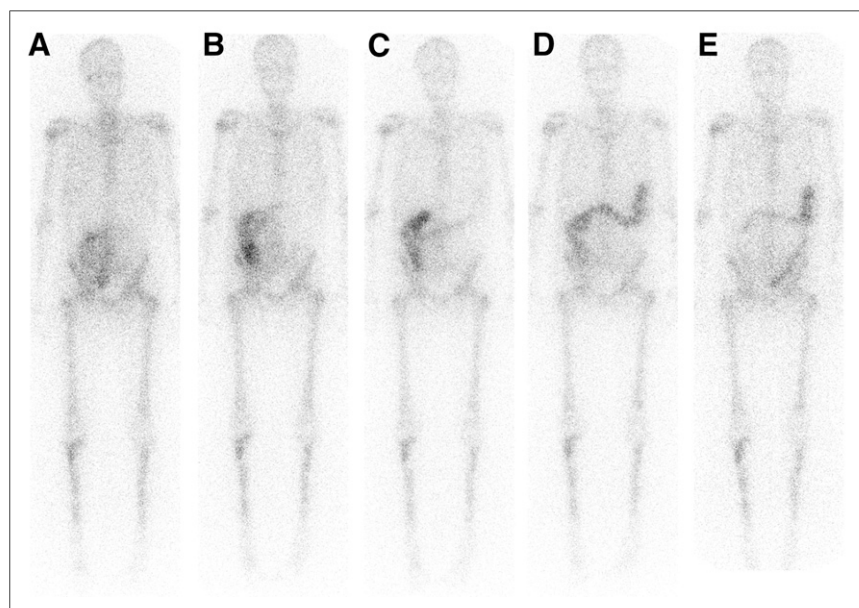


FIGURE 1. Whole-body anterior images for patient 3 acquired at 4 (A), 24 (B), 48 (C), 72 (D), and 144 h (E) after administration.

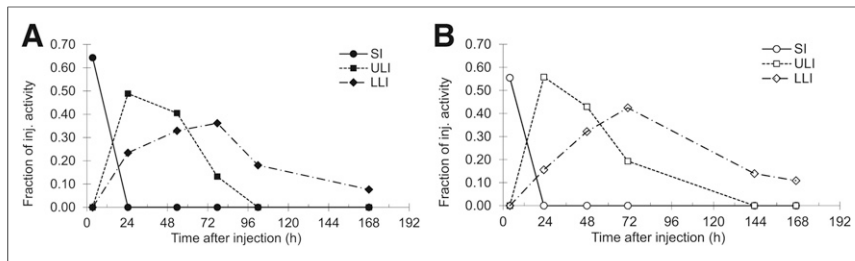


FIGURE 2. Activity retention curves in SI, ULI, and LLI for patient 1 for administration 1 (A) and administration 2 (B). inj = injected.

Measurements were taken immediately after injection, before first void, and then at 1 h and thereafter every 2 h during the first day, then at least twice daily until discharge. Subsequent measurements were taken at 96 and 144 h after injection.

γ -Camera Imaging. Scans were performed on the Philips Forte γ camera using the medium-energy general-purpose collimator according to a protocol previously detailed (16). Because there was an insufficient counting rate to acquire SPECT data in a time frame that was comfortable for the patient, whole-body and spot views were acquired for approximately 30 min each, using matrix sizes of $256 \times 1,024$ and 256×256 pixels, respectively. Imaging was performed using an energy window set at 82 keV with a 20% width to encompass counts from the 81- and the 84-keV emissions from ^{223}Ra . The first scan was acquired within 0–4 h after injection, and subsequent scans were acquired at 24, 48, 96, and 144 h after injection. All images were acquired after voiding to reduce artifacts due to radioactivity in the bladder. The counting rate for all measurements was sufficiently low (<1 kcts/s over the entire spectrum counted by the camera) such that no correction was required for detector dead-time for any scans. Quantification and attenuation correction were performed as previously detailed (16).

Dosimetry

Regions of interest were delineated on the images over bone uptake with reference to the $^{99\text{m}}\text{Tc}$ -methylene diphosphonate bone scans acquired at pretreatment assessment. Activity in bone was calculated as the mean of

the activity per unit mass in the right and left legs and skull, to avoid difficulties in interpretation due to gut and lesion uptake in the torso. The activity in bone was assumed to be distributed on the cortical and trabecular bone surfaces, in a ratio relative to the total bone surface (38% on cortical bone surfaces and 62% on trabecular bone) (20,21).

The activity in the red marrow was calculated from the blood sample measurements assuming a blood-to-bone marrow activity concentration ratio of 1.0 (22). The red marrow absorbed doses from activity on the bone surfaces and

from blood were calculated separately.

No specific uptake was seen in the kidneys on the whole-body scans. The cumulated activity in the kidneys was therefore calculated from the kidney mass and measurements of the concentration of activity excreted in the urine. The activity in the urine over the first collection period (0 to ~2 h after injection) was taken to be the activity measured at the end of this period. The activity in each subsequent collection was taken to be the average of the activity measured at the start and end of the collection period. The effective half-life after the last collection was extrapolated from the final data points. The cumulated activity in the bladder was calculated from the activity concentration determined from the collected urine.

The cumulated activity in the gut was derived from regions of interest drawn over the areas of gut uptake on the whole-body scans. In keeping with ICRP 100, the contribution of the α emission to the gut wall from the contents was taken to be 0 (23).

No specific uptake was seen in the liver on the whole-body scans. The activity in the liver was therefore estimated from the activity concentration measured in blood, under the worst-case assumption that the liver was entirely composed of blood. The blood activity concentration was multiplied by the mass of the liver to give an upper value of the activity in the liver at each time point.

The cumulated activity in the whole body was calculated from the patient’s counts measured on the low-sensitivity whole-body counter.

For imaged organs, cumulated activities were calculated by trapezoidal integration. The activity at time zero was assumed to

TABLE 2
Mean Residence Times and Absorbed Doses Delivered from Both Administrations

Organ	Mean residence time (h)	α absorbed dose (mGy/MBq)		$\beta + \gamma$ absorbed dose (mGy/MBq)	
		Mean	Range	Mean	Range
SI wall	6.8	0	NA	5	3–10
ULI wall	29.2	0	NA	38	6–68
LLI wall	29.2	0	NA	61	5–176
Kidneys	0.1	6	2–15	<1	—
Red marrow, from blood	0.2	2	1–5	<1	—
Red marrow, from bone surfaces	—	408	177–994	9	4–22
Bone surfaces	97.0	5,378	2,331–13,118	21	9–51
Liver	0.3	2	1–5	<1	—
Urinary bladder wall	0.1	3	1–8	<1	—
Total body	154.8	29	14–66	1	1–3

NA = not applicable.

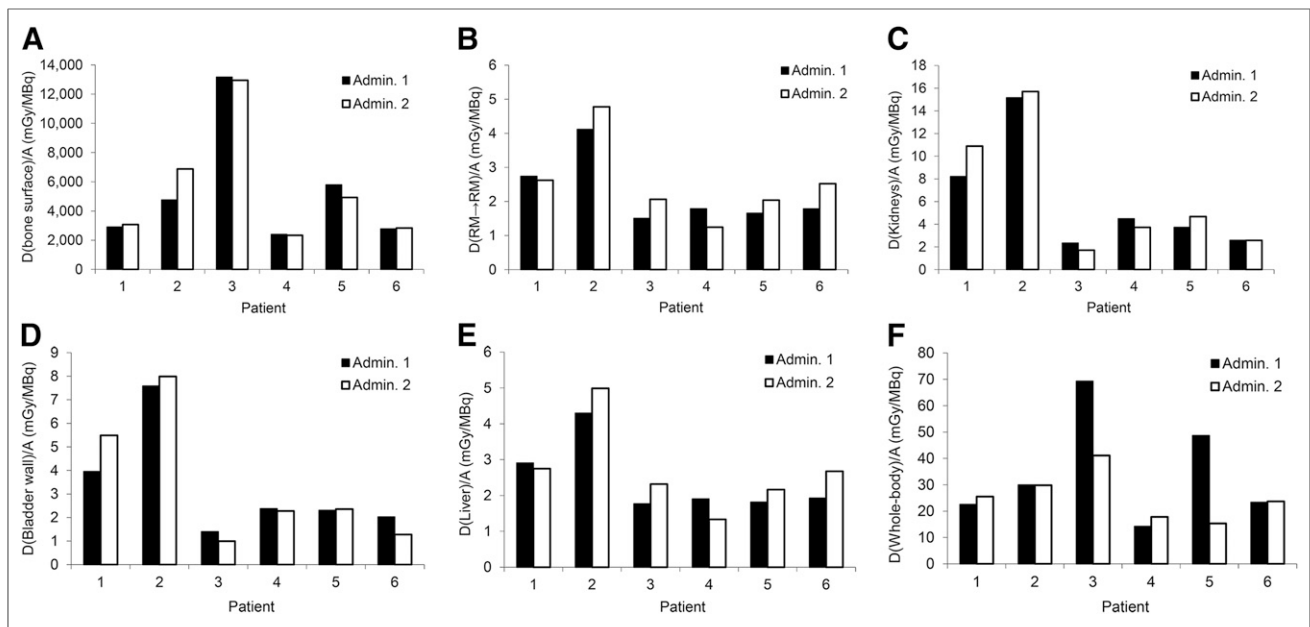


FIGURE 3. Absorbed dose (in mGy/MBq) for bone surfaces (A), red marrow from blood (B), kidneys (C), bladder wall (D), liver (E), and whole body (F). Admin. = administration.

equal the activity at the first image. The effective half-life as determined from the last 2 γ -camera images was used for extrapolation from the last measurement to infinity.

The absorbed doses delivered to normal organs were calculated with Olinda/EXM with an α quality-weighting factor of 1 (24,25). Patient-specific mass corrections were made to the Olinda S values for the whole body but not for other organs because of insufficient anatomic information for accurate mass determination. The total absorbed dose to the target region was calculated as the sum of the contributions from all source regions and included contributions from the decay of the daughter products of ^{223}Ra .

Statistical Analysis

A statistical comparison was made between the inpatient absorbed doses delivered at both administrations using the combined data from a representative organ for each method of data acquisition—that is, whole-body (external patient counting), liver (blood sampling), kidneys (excretion sample counting), and bone surfaces (quantitative imaging). A correlation coefficient and corresponding *P* value were calculated. Bladder wall absorbed doses were excluded from the comparison because they were derived from the same sample measurements as the kidney doses (i.e., the activity concentration in urine). Similarly, red marrow doses were excluded because they were derived from bone surface uptake and blood activity measurements. No absorbed dose comparisons were made in the case of the gut as no correspondence was expected because of differing excretion patterns after each administration.

Statistical analysis was performed using GraphPad Prism (GraphPad Software). The D'Agostino–Pearson test was used for normality. A statistically significant *P* value was considered to be less than 0.05. Descriptive statistics are presented either as mean \pm SD, where data are normally distributed, or as median with the range. Mean or median absorbed doses are given as an average over all patients and both administrations.

RESULTS

Baseline and treatment characteristics for the 6 patients enrolled in the study are given in Table 1.

Pharmacokinetics and Biodistribution

The injected activity cleared rapidly from the blood, with 1.1% (range, 0.6%–5.1%) remaining at 24 h.

Specific uptake was seen on the γ -camera images in the whole body, bone, and gut (Fig. 1). Most of the administered activity was taken up rapidly into bone, with $61\% \pm 10\%$ in the bone on the first scan 4 h after injection.

Activity passed rapidly into the small intestine (SI). For all patients, the maximum SI uptake had already occurred by the time of the first scan. At 4 h, $40\% \pm 19\%$ of the administered activity was in the SI, and by 72 h all activity had cleared the SI. The maximum activity uptake in the upper large intestine (ULI) was $45\% \pm 16\%$ at 24 h, decreasing to 4% (range, 0%–18%) at 1 wk. The maximum uptake in the lower large intestine (LLI) occurred at 24–72 h, with an uptake of $17\% \pm 11\%$ at 48 h decreasing to $6\% \pm 4\%$ at 1 wk after administration. Figure 2 shows an example of the transit of the activity through the gut.

Fecal excretion was the main route of elimination of activity from the body. Cumulative fecal excretion was $13\% \pm 12\%$ at the time of discharge (~ 48 h after injection). Excretion of activity in the urine was significantly lower than that in feces. At discharge, cumulative urine excretion was $2\% \pm 2\%$ of the injected activity, and the rate of activity excretion was decreasing in all cases.

Dosimetry

The absorbed doses per injected activity delivered to each organ are summarized in Table 2 and displayed in Figure 3. It can be seen that the whole-body dose delivered from the second administration is within 30% of that delivered from the first, with the exception of 2 cases for which fecal excretion patterns differed. A statistical comparison between the inpatient absorbed doses from the 2 administrations for the bone surfaces, kidneys, liver, and whole-body resulted in a correlation coefficient of 0.99 ($P < 0.01$), indicating a significant correspondence between the absorbed doses delivered at the 2 administrations. In contrast, the interpatient variability in the delivered absorbed doses per injected activity varied from

TABLE 3
Incidence of Adverse Events

Adverse event: system organ class preferred term	No. of patients (%)	Highest common toxicity criteria grade (no. of patients)	Relationship to ²²³ Ra dichloride: term (no. of patients)
Any adverse event	6 (100.0)	—	—
Gastrointestinal disorders	4 (66.7)	—	—
Nausea	2 (33.3)	1 (2)	Possible (2)
Abdominal discomfort	1 (16.7)	1 (1)	Possible (1)
Constipation	1 (16.7)	1 (1)	Unlikely (1)
Diarrhea	1 (16.7)	—*	Probable (1)
Musculoskeletal and connective tissue disorders	3 (50.0)	—	—
Bone pain	2 (33.3)	1 (2)	Unlikely (1) Probable (1)
Back pain	1 (16.7)	1 (1)	Unlikely (1)
Blood and lymphatic system disorders	1 (16.7)	—	—
Anemia	1 (16.7)	2 (1)	Possible (1)
General disorders and administration site conditions	3 (50.0)	—	—
Chest pain	1 (16.7)	3 (1)	Possible (1)
Disease progression	1 (16.7)	5 (1)*	Unlikely (1)
Fatigue	2 (33.3)	1 (2)	Unlikely (1) Possible (1)
Infections and infestations	1 (16.7)	—	—
Urinary tract infection	1 (16.7)	2 (1)	Unlikely (1)
Metabolism and nutrition disorders	1 (16.7)	—	—
Anorexia	1 (16.7)	—†	Possible (1)

*One patient died approximately 1 y after first administration, due to disease progression.

†No common toxicity criteria grade reported; severity was recorded as mild, defined as transient and easily tolerated.

a minimum of 150% for the liver absorbed dose to nearly 400% for the bone surfaces and red marrow.

Safety

All 6 patients experienced an adverse event during the study (Table 3). The most frequently reported adverse events were gastrointestinal (4 patients, 66.7%) and musculoskeletal and connective tissue disorders (3 patients, 50%).

DISCUSSION

The pharmacokinetic results of this trial demonstrated that the ²²³Ra-dichloride was rapidly cleared from the blood and taken up into bone, which supports previous findings (8,12). The main route of excretion was via the feces. The mechanism of transport from the blood into the SI is not currently understood but clearly took place rapidly because the maximum uptake in the SI had already occurred by the time of the first scan 4 h after administration as has been previously observed (12). Subsequent activity levels in the SI fell sharply, and activity appeared to pass into the LLI via the ULI.

It was assumed that the localization of all daughter products followed that of the ²²³Ra. However, as stated in ICRP 67 (26) it is possible that ²¹¹Pb (with a half-life of 36 min) may localize to liver, although the γ emissions from this daughter product are at the extreme

of the range of the γ camera. The potential for ²¹¹Bi (with a half-life of 5 min) to localize in liver was explored by Carrasquillo et al. (12) by imaging of the 351-keV emission, with inconclusive results.

The biologic effect of absorbed doses received from α particles is poorly understood in a therapeutic context (27). Thus, although radiation weighting factors ranging from 5 to 20 are often applied to evaluate stochastic risks due to the high linear energy transfer of the emissions, for this study no weighting factor was applied.

With the exception of the gastrointestinal tract, the mean absorbed doses for each organ presented in Table 2 vary by up to an order of magnitude. The absorbed doses previously calculated based on ICRP models (18) fall within these ranges except for the red marrow, bone surfaces, and liver. Similar absorbed doses were delivered to the gastrointestinal tract although the major contribution demonstrated by Lassmann and Nosske (18) is from α irradiation, whereas this was set to 0 for this study according to the later ICRP model (23). The upper range of absorbed doses delivered to the red marrow and bone endosteum in this study are significantly higher (by up to a factor of 14) than those of Lassmann and Nosske (18). The absorbed dose to the liver was found to be significantly lower in this study.

In this study, mild adverse myelotoxicity was seen for only 1 patient, although anemia, leukopenia, neutropenia, and thrombo-

cytopenia have been reported in other studies (8–13). Adverse myelotoxicity has not been seen at a level that might be expected from the high total absorbed doses determined in this study. Absorbed doses are primarily delivered to the red marrow from circulating blood and from uptake on the bone surfaces. However, α emissions will irradiate only a small fraction of the red marrow because of their short range (28). The absorbed dose delivered from the circulating activity may therefore be a more relevant guide to the potential for marrow toxicity than that due to activity on the bone surfaces. The large self-absorbed doses delivered to the bone surfaces are particularly of note and may prove in the long term to be the cause of dose-limiting toxicity.

Calculations of the mean absorbed dose delivered to the walls of the SI, ULI, and LLI were performed under the assumptions that all the activity was in the gut contents and that the contribution to the walls of the gut from α emissions was negligible, as stated by ICRP 100 (23). Although acute gastrointestinal toxicity from ^{223}Ra -dichloride treatment has not been reported as a significant occurrence in other studies, diarrhea has been reported and indeed 1 patient in this study experienced diarrhea (8–13). If ^{223}Ra is retained in the mucosa, the absorbed dose delivered to the walls of the gut may not be negligible and the above assumptions would result in an underestimation of gut doses.

Whole-body dosimetry can be calculated accurately and has proven to be a reliable surrogate for the absorbed dose delivered to the red marrow in studies of ^{131}I -metaiodobenzylguanidine therapy (29). The relative simplicity of this procedure also facilitates its routine clinical use. However, a key assumption for organ-level dosimetry is uniform distribution of uptake, and only an average absorbed dose is calculated for a target organ. These assumptions are particularly erroneous for treatment with α emitters, and whole-body dosimetry may prove to be of limited value. Further studies are required to investigate this.

Interpatient comparisons indicate that a wide range of absorbed doses are delivered from weight-based administrations of activity whereas intrapatient results show that the absorbed doses delivered from a second administration closely follow those delivered from the first in most cases. Taken into consideration with the generally low-toxicity profile of the studies performed to date, the implication is that the option of personalized treatments could be explored.

CONCLUSION

This dosimetry study of ^{223}Ra -dichloride has demonstrated a range of absorbed doses delivered to critical organs. Biodistribution, pharmacokinetics, and absorbed doses are largely consistent over 2 administrations for any given patient, which would facilitate personalized treatments.

DISCLOSURE

The costs of publication of this article were defrayed in part by the payment of page charges. Therefore, and solely to indicate this fact, this article is hereby marked “advertisement” in accordance with 18 USC section 1734. Research funding was provided by Bayer Healthcare Pharmaceuticals and Algeta ASA. Christopher C. Parker consults for Bayer Healthcare Pharmaceuticals and Algeta ASA. NHS funding was provided to the NIHR Biomedical Research Centre at The Royal Marsden and the ICR. Valerie J. Lewington consults for Bayer Healthcare Pharmaceuticals. No other potential conflict of interest relevant to this article was reported.

REFERENCES

1. Lange PH, Vasella RL. Mechanisms, hypotheses and questions regarding prostate cancer metastatic to bone. *Cancer Metastasis Rev.* 1998–1999;17:331–336.

2. Sartor O. Radiopharmaceutical and chemotherapy combinations in metastatic castrate-resistant prostate cancer: a new beginning. *J Clin Oncol.* 2009;27:2417–2418.
3. Petrylak DP, Tangen CM, Hussain MH, et al. Docetaxel and estramustine compared with mitoxantrone and prednisone for advanced refractory prostate cancer. *N Engl J Med.* 2004;351:1513–1520.
4. Tannock IF, de Wit R, Berry WR, et al. Docetaxel plus prednisone or mitoxantrone plus prednisone for advanced prostate cancer. *N Engl J Med.* 2004;351:1502–1512.
5. Muralidharan A, Smith MT. Pathobiology and management of prostate cancer-induced bone pain: recent insights and future treatments. *Inflammopharmacology.* 2013;21:339–363.
6. Henriksen G, Fisher DR, Roeske JC, et al. Targeting of osseous sites with α -emitting ^{223}Ra : Comparison with the β -emitter ^{89}Sr in mice. *J Nucl Med.* 2003;44:252–259.
7. Ritter MA, Cleaver JE, Tobias CA. High-LET radiations induce a large proportion of non-rejoining DNA breaks. *Nature.* 1977;266:653–655.
8. Nilsson S, Larsen RH, Foss SD, et al. First clinical experience with α -emitting radium-223 in the treatment of skeletal metastases. *Clin Cancer Res.* 2005;11:4451–4459.
9. Nilsson S, Franzen L, Parker C, et al. Bone-targeted radium-223 in symptomatic, hormone-refractory prostate cancer: a randomised, multicentre, placebo-controlled phase II study. *Lancet Oncol.* 2007;8:587–594.
10. Nilsson S, Strang P, Aksnes A, et al. A randomized, dose-response, multicentre phase II study of radium-223 chloride for the palliation of painful bone metastases in patients with castration-resistant prostate cancer. *Eur J Cancer.* 2012;48:678–686.
11. Parker CC, Pascoe S, Chodacki A, et al. A randomized, double-blind, dose-finding, multicentre, phase 2 study of radium chloride ($\text{Ra}223$) in patients with bone metastases and castration-resistant prostate cancer. *Eur Urol.* 2013;63:189–197.
12. Carrasquillo JA, O'Donoghue JA, Pandit-Taskar N. Phase I pharmacokinetic and biodistribution study with escalating doses of ^{223}Ra -dichloride in men with castration-resistant metastatic prostate cancer. *Eur J Nucl Med Mol Imaging.* 2013;40:1384–1393.
13. Parker C, Nilsson S, Heinrich D, et al. Alpha emitter radium-223 and survival in metastatic prostate cancer. *N Engl J Med.* 2013;369:213–223.
14. Sartor O, Coleman R, Nilsson S, et al. Effect of radium-223 dichloride on symptomatic skeletal events in patients with castration-resistant prostate cancer and bone metastases: results from a phase 3, double-blind, randomised trial. *Lancet Oncol.* 2014;15:738–746.
15. Henriksen G, Bristol K, Bruland OS, Fodstad O, Larsen RH. Significant antitumor effect from bone-seeking, alpha-particle-emitting ^{223}Ra demonstrated in an experimental skeletal metastases model. *Cancer Res.* 2002;62:3120–3125.
16. Hindorf C, Chittenden S, Aksnes A-K, Parker C, Flux GD. Quantitative imaging of ^{223}Ra -chloride (Alpharadin) for targeted alpha-emitting radionuclide therapy of bone metastases. *Nucl Med Commun.* 2012;33:726–732.
17. Bruland ØS, Nilsson S, Fisher DR, et al. High-linear energy transfer irradiation targeted to skeletal metastases by the α -emitter ^{223}Ra : adjuvant or alternative to conventional modalities? *Clin Cancer Res.* 2006;12(20 Pt 2, suppl):6250s–6257s.
18. Lassmann M, Nosske D. Dosimetry of ^{223}Ra -chloride: dose to normal organs and tissues. *Eur J Nucl Med Mol Imaging.* 2013;40:207–212.
19. Oken MM, Creech RH, Tormey DC, et al. Toxicity and response criteria of the Eastern Cooperative Oncology Group. *Am J Clin Oncol.* 1982;5:649–655.
20. International Commission on Radiological Protection (ICRP). *Limits for Intakes of Radionuclides by Workers.* ICRP publication 30 (part 1). Oxford, U.K.: ICRP; 1979.
21. International Commission on Radiological Protection (ICRP). *Basic Anatomical and Physiological Data for Use in Radiological Protection: The Skeleton.* ICRP publication 70. Oxford, U.K.: ICRP; 1995.
22. Hindorf C, Glatting G, Ciesca C, et al. EANM Dosimetry Committee guidelines for bone marrow and whole-body dosimetry. *Eur J Nucl Med Mol Imaging.* 2010;37:1238–1250.
23. International Commission on Radiological Protection (ICRP). *Human Alimentary Tract Model for Radiological Protection.* ICRP publication 100. Oxford, U.K.: ICRP; 2006.
24. Stabin MG, Siegel JA. Physical models and dose factors for use in internal dose assessment. *Health Phys.* 2003;85:294–310.
25. Stabin MG, Sparks RB, Crowe E. OLINDA/EXM: the second-generation personal computer software for internal dose assessment in nuclear medicine. *J Nucl Med.* 2005;46:1023–1027.
26. International Commission on Radiological Protection (ICRP). *Age-Dependent Doses to Members of the Public from Intake of Radionuclides: Part 2 Ingestion Dose Coefficients.* ICRP publication 67. Oxford, U.K.: ICRP; 1992.
27. Sgouros G, Roeske JC, McDevitt MR, et al. MIRD pamphlet no. 22 (abridged): radiobiology and dosimetry of alpha-particle emitters for targeted radionuclide therapy. *J Nucl Med.* 2010;51:311–328.
28. Hobbs RF, Song H, Watchman CJ, et al. A bone marrow toxicity model for ^{223}Ra α -emitter radiopharmaceutical therapy. *Phys Med Biol.* 2012;57:3207–3222.
29. Buckley SE, Chittenden SJ, Saran FH. Whole-body dosimetry for individualized treatment planning of ^{131}I -MIBG radionuclide therapy for neuroblastoma. *J Nucl Med.* 2009;50:1518–1524.